Proceedings of the American Control Conference
San Diego, California • June 1999

Dynamic Control of Permanent Magnet Synchronous Motors for Automotive Drive Applications.

Paul Stewart, Visakan Kadirkamanathan.
Department of Automatic Control and Systems Engineering
UNIVERSITY OF SHEFFIELD Mappin St. Sheffield S1 3JD, UK

Abstract

Due to factors such as high power density and efficiency, low torque ripple and maintenance, and extremely wide operating speed range, permanent magnet AC motors (PMAC) are the subject of intense development for traction drive applications. Maximum torque production for both traction performance and electronic gearchanging requires the operating condition to be as close to voltage saturation as possible in the flux weakening region. A fully dynamic model reference flux-weakening controller with feedback linearisation decoupling is presented, which allows the maximum torque-speed trajectory to be followed dynamically, without saturation of the current controllers.

1 Introduction

The surface mounted permanent magnet AC motor operates under two distinct regimes, namely constant torque, and constant power. The boundary between these modes (base speed) is defined by operating conditions where the magnitude of the applied voltage equals the magnitude of the back emf. The motor under consideration is three phase with a "smooth" rotor with surface mounted magnets, and sinusoidal emf.

The constant torque operation of the PMAC is not a novel subject area [1], [2]. Instantaneous torque control is achieved via current vector control in a transformed orthogonal reference frame. For the PMAC surface mount machine, the d-axis current is controlled to zero to ensure maximum torque-per-amp operation. In order to extend the range of the machine beyond base speed, the performance degradation associated with current regulator saturation must be addressed allowing smooth transition into the constant power region. A series of developments based upon the onset of current errors evolved to enable the extended speed region via the injection of negative d-axis current [3].

The algorithms are extensions of basic feedforward control techniques [4] [5]. Current regulator saturation is detected by increasing errors in the d-axis current, which is very small in the constant power region due to high current regulator gains. The error detection serves to suppress the q-axis current command thus regaining at least partial control of the current vector. Steady-state experimental performance confirms the flux-weakening capability of this class of controllers. However, since phase-advance is actuated by current controller saturation, insufficient voltage headroom exists to allow the current vector to *dynamically* follow the maximum torque envelope.

A more sophisticated approach [6], [7], [8] has been developed which unlike earlier methods does not rely upon current or voltage feedback from the motor to calculate the appropriate level of d and q-axis current for flux weakening, relying instead on known machine parameters to perform the necessary calculations. The d and q-axis current commands are derived either by real-time solution, or by look-up table, of the steady-state system equations. These methods are shown to provide good performance in the flux-weakening region, and under steady-state conditions achieve the maximum torque-per-amp profile. Since the dynamic current components are neglected in the calculation of current commands, no voltage headroom is available to optimally advance the current vector under dynamic conditions. The subsequent degradation in current performance is particularly significant under dynamic no-load conditions such as gear-changing.

In this paper, a dynamic model reference controller is presented, which reserves an appropriate amount of inverter voltage to allow the maximum possible torque-speed envelope to be followed under dynamic conditions. State de-coupling is achieved by a non-linear feedback element, and losses reduced in the region below the maximum torque envelope by minimising the magnitude of the current vector at all times.

For automotive drives applications, this results in maximum performance, and the shortest possible gear change times via an electronically actuated gearbox.

0-7803-4990-6/99 $10.00 © 1999 AACC

2 PMAC Motor Principles

The stator windings of the motor are distributed to give a sinusoidal emf with the three phase currents having a separation of 120^0 electrical.
The d-q transformation [6] is applied to transform the three phase currents into an orthogonal reference frame rotating synchronously with the rotor flux. Where V_d,V_q are the d and q axis voltages, i_d,i_q are the d and q axis currents, r is the phase resistance, ω is the rotor velocity, L the phase inductance and λ the back emf constant.

$$V_q = r\, i_q + \omega\, L\, i_d + \omega\, \lambda + \mathrm{L}\left(\frac{di_q}{dt}\right) \tag{1}$$

$$V_d = r\, i_d - \omega\, L\, i_q + \mathrm{L}\left(\frac{di_d}{dt}\right) \tag{2}$$

The system equations operate subject to the constraints (eq:3) on voltage and current, where V is the magnitude of the voltage vector, and I is the magnitude of the current vector. Considering the system constraints, maximum torque-per-amp operation below base speed requires the d-axis current to be controlled to zero. Above this boundary, the rising emf value can be countered by advancing the current vector with respect to the rotor, and introducing negative d-axis current

$$V^2 \geq {V_q}^2 + {V_d}^2,\ I^2 \geq {i_q}^2 + {i_d}^2 \tag{3}$$

The requirements of the flux weakening controller are to calculate the velocity at which flux-weakening is to be initiated, and to output optimal d and q-axis current commands in steady-state and dynamic operation. The most convenient description of the system is the steady-state circle diagram, in the d-q reference frame. If resistance is neglected, then from (eq:1),(eq:2) the steady-state system becomes (eq:4),(eq:5), and the instantaneous torque (T_e) for the surface mount PMAC motor is given by (eq:6), where k_t is the motor torque constant.

$$V_q = \omega\, L\, i_d + \omega\, \lambda \tag{4}$$

$$V_d = -\omega\, L\, i_q \tag{5}$$

$$T_e = k_t\, i_q \tag{6}$$

In the phasor diagram complex plane, the current is limited to a circular locus given by (eq:3). Similarly, the maximum available inverter voltage limits the current vector to a circular locus with frequency dependant radius, and different centre $\left(\frac{-\lambda}{L}\right)$. The voltage limit locus is derived from the identity (eq:3), then in steady-state;

$$V^2 = \omega^2\, L^2\, {i_q}^2 + (\omega\, \lambda + \omega\, L\, i_d)^2 \tag{7}$$

and;

$$\frac{V}{\omega\, L} = \sqrt{{i_q}^2 + \left(i_d + \frac{\lambda}{L}\right)^2} \tag{8}$$

The graphical representation (fig:1) shows the important control principles. For maximum torque-per-amp operation, the current vector is aligned with the q-axis until base speed. Subsequently, the current vector follows the intersection between the current and voltage locii. In order to minimise I^2r losses an extra constraint is that for all torque demands below the maximum torque envelope, the magnitude of the current vector must be minimised.

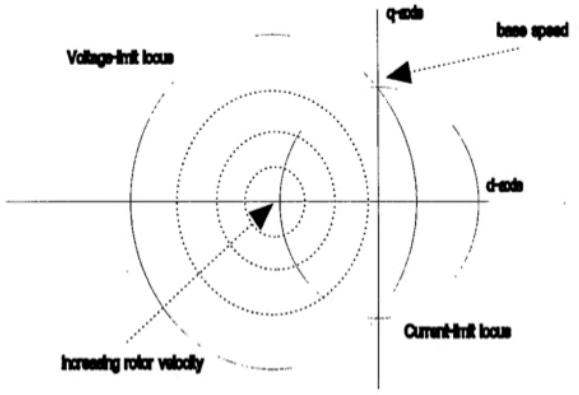

Figure 1: PMAC motor circle diagram showing constraint locii.

3 Model Reference Control

A geometrical representation of (fig:1) the steady-state system can be derived from the system equations (eq:7) (eq:8), and used as a model reference to provide command values to d-axis and q-axis current controllers [9]. In order to achieve tracking of the model reference command values in dynamic mode, and to reduce torque ripple from high feedback gains, feedback linearisation is applied to design a controller to replace conventional PID current controllers.

3.1 Feedback Linearisation

The PMAC motor system equations are cross-coupled, and bi-linear in the states. Non-linear feedback elements are designed [10], such that accurate tracking of current command signals is achieved (eq:9),(eq:10).

$$V_d = r\, i_d - \omega\, L\, i_q + V_1\, L \tag{9}$$

$$V_q = r\, i_q + \omega\, L\, i_d + \lambda\omega + V_2\, L \tag{10}$$

A controller is designed [11] where auxilliary inputs (eq:11),(eq:12) are substituted into the non-linear feedback elements. Decoupling of the current loops is achieved, resulting in improved current regulator control, and consequently accurate tracking of the model reference command trajectories.

$$V_1 := \frac{d\, i_d^*}{dt} + k\, i_d^* - k\, i_d \tag{11}$$

$$V_2 := \frac{d\, i_q^*}{dt} + k\, i_q^* - k\, i_q \tag{12}$$

Which results in error dynamics of;

$$\frac{d\underline{e}}{dt} + k\underline{e} = 0 \tag{13}$$

Where;

$$\underline{e} = \begin{bmatrix} i_d^* - i_d \\ i_q^* - i_q \end{bmatrix} \tag{14}$$

4 Dynamic Extension to the Model Reference Controller

Examination of the full system dynamic equations (eq:1) (eq:2) shows an unmodelled voltage drop V_{dr} due to the advance of the current vector under flux weakening, whose magnitude is given by (eq:15);

$$V_{dr} = \sqrt{\left(\frac{di_d\, L}{dt}\right)^2 + \left(\frac{di_q\, L}{dt}\right)^2} \tag{15}$$

The purpose of the model reference dynamic extension is to include the motor current dynamics, so that the controller embodies a complete description of the PMSM system equations. This extension is achieved by deriving a set of equations for the rate of change of phase of the current vector in the d-q reference frame. Once this derivation is complete, the terms are used in the model reference controller to reserve supply voltage to allow the current dynamics to operate without saturation of the current controllers. A new base speed is calculated to switch in this compensation. Differentiating the voltage locus identity (eq:7) gives an expression which is solved for $\left(\frac{d\alpha}{dt}\right)$ and simplified to give a term which describes the current vector dynamics in the flux-weakening region (eq:16), where α is the current vector advance angle.

$$\left(\frac{d\alpha}{dt}\right) = -\frac{k_t\,(L^2\, I^2 + 2\, L\, I \sin(\alpha)\, \lambda + \lambda^2)}{\omega\, \lambda\, L\, J} \tag{16}$$

The dynamic term (eq:16) can now be included in the model reference controller using the substitutions in (eq:17) to calculate the voltage drop (V_{dr}) (eq:18) due to the current phase dynamics .

$$\left(\frac{di_q}{dt}\right) = -i_d \left(\frac{d\alpha}{dt}\right), \left(\frac{di_d}{dt}\right) = i_q \left(\frac{d\alpha}{dt}\right) \tag{17}$$

$$V_{dr} = \frac{k_t LI\,(L^2\, I^2 + 2\, L\, I \sin(\alpha)\, \lambda + \lambda^2)}{\omega\, \lambda\, L\, J} \tag{18}$$

The steady state model reference can now be extended to include the dynamic terms. The dynamic compensated term can be visualised as a voltage frequency circle leading the steady state voltage frequency constraint circle by an amount proportional to the dynamic voltage drop. This term must be switched in at an appropriate base speed, since the dynamic compensation term (eq:18) is valid only under field weakening conditions.

4.1 Base Speed Under Dynamic Conditions

It is necessary to switch in the dynamic compensation at a base speed appropriate to the new model reference. Base speed occurs at a lower rotor velocity than in the steady state due to the voltage which is reserved to allow the current phase dynamics. At this new base speed, which is the boundary of the field weakening region. the d-axis current is set to zero, and equation (eq:18) reduces to (eq:19);

$$V_{dr} = \frac{L\, I\, \mathrm{k_t}(L^2\, I^2 + \lambda^2)}{\omega\, \lambda\, J} \tag{19}$$

An alternative expression is derived from (eq:8), which links the difference between the magnitudes of the voltage frequency circles at dynamic and steady state base speeds (eq:20).

$$V_{drop} = V - \sqrt{I^2 + \frac{\lambda^2}{L^2}}\, \omega\, L \tag{20}$$

$$0 = -\sqrt{I^2 + \frac{\lambda^2}{L^2}}\, \omega^2\, L + V\, \omega - \frac{L\, I\, \mathrm{k_t}(L^2\, I^2 + \lambda^2)}{\lambda\, J} \tag{21}$$

Combining (eq:19) and (eq:20) results in a quadratic in rotor velocity (eq:21), one solution gives the difference between dynamic and steady state base speed, the other solution gives the dynamic base speed. The dynamic voltage compensation in the model reference controller can now be switched in and out at the appropriate rotor velocity.

5 Performance Comparisons

The experimental and simulation derivations are based upon a three-phase PMAC traction motor.
Winding: Three phase star connected.
Generated voltage: Sinusoidal.
Phase mutual inductance: 59μH.
Phase self inductance: 118μH.
Phase resistance: $2.46\text{m}\Omega$.
Pole number: 8.
Torque constant k_t: $0.48Nm/A_{rms}$.
Phase emf constant λ: $0.26V/Rad/Second$.
DC voltage: $240V_{dc}$.
Current limit: $354A_{rms}$. As the rotor velocity corresponding to the dynamic base speed is reached, the dynamic voltage drop is calculated, and subtracted from the value of supply voltage being supplied to the model reference. By this method, an appropriate amount of voltage is reserved for the current vector dynamics, allowing flux weakening to progress while maintaining the current controllers just within the bound of saturation. The dynamic extension to the model reference controller defines a new base speed appropriate to the *dynamic* operating conditions. By sacrificing a small amount of the torque envelope below base speed, current control is maintained resulting in enhanced performance by the dynamic controller above steady state base speed (fig:2). The torque envelope of the dynamic controller is also considerably smoother. D axis current is injected earlier by the compensated controller, which results in the magnitude of the supplied voltage rising smoothly to just below saturation. Thus the current vector is controlled at all times.

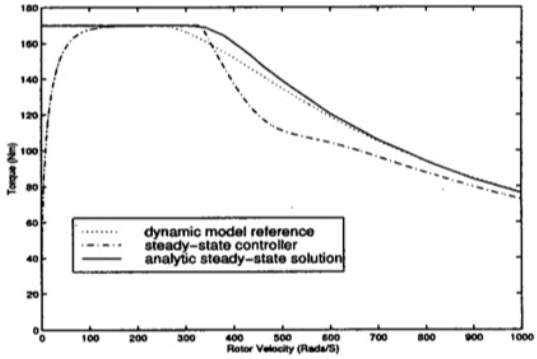

Figure 2: Steady-state analytic solution under steady-state conditions, steady-state model reference, and dynamic model reference under dynamic conditions.

6 Conclusion and Future Work

A control method has been presented which extends existing techniques of control, to make available an enhanced torque speed envelope for the PMAC motor. This enhancement is advantageous for electric vehicle traction drives, both for performance and gear shifting.

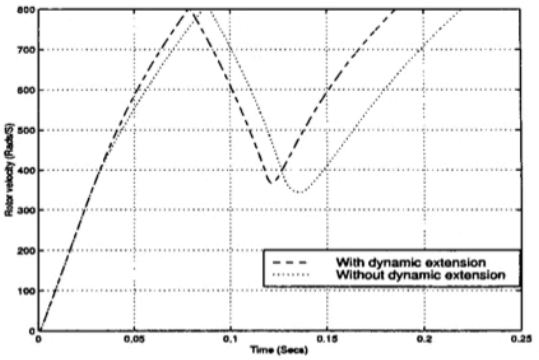

Figure 3: Performance assessment:velocity profiles of PMSM driving two-speed gearbox, with/without dynamic compensation.

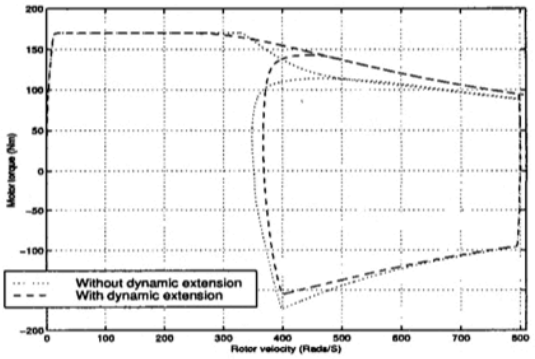

Figure 4: Performance assessment:torque profiles of PMSM machine driving two-speed gearbox, with/without dynamic compensation.

The system is simulated as a motor seeing an external load torque via a two speed gearbox with ratios of 2:1, and 1:1. The simulation method is as follows:
The motor is driving into a 40 Nm external load.
The motor accelerates to a rotor velocity of 800 rad/s, constituting an output velocity of 400 rad/s and a distubance torque of 20Nm via a 2:1 gearbox ratio.
At a rotor velocity of 800 rad/s, torque output is reduced to zero to allow the 2:1 gear to be disengaged.
The motor is decelerated to 400 rad/s, to match the output shaft velocity via a 1:1 gearbox ratio.
At a rotor velocity of 400 rad/s, torque output is re-

duced to zero to allow the 1:1 gear to be engaged. The motor accelerates to a rotor velocity of 800 rad/s, constituting an output velocity of 800 rad/s and a disturbance torque of 40 Nm vis the 1:1 gearbox ratio. The motor performance assessment (figs:4,3) shows both the two quadrant operation of the system (fig:4), and the velocity profile (fig:3) which exhibits a 16 percent advantage in favour of the system with the dynamic extension in completing the profile. It must be borne in mind that most of the components of the calculations for switching the dynamic base speed, and calculating the dynamic voltage drop already exist in the steady state controller. As a physical implementation, the results of these components reside in memory addresses. The implementation in DSP thus requires only manipulation of existing calculation results, and the effort involved in extending the implementation is justifiable when considering the benefits in terms of robustness and performance. Future work on the PMAC motor controller includes a study of the system robustness, inclusion of the controller action into the model reference, parameter and state estimation.

References

[1] T.M.Jahns, G.B.Kliman, and T.W.Neumann, "Interior permanent magnet synchronous motors for adjustable speed drives," *IEEE Trans. Ind. Appl.*, vol. IA-22, pp 738-747, July/Aug. 1986.

[2] P.Pillay, and R.Krishnan, "Modeling, simulation, and analysis of permanent magnet motor drives. Part I: The permanent-magnet synchronous motor drive," *IEEE Trans. Ind. Appl.*, vol. IA-25, pp 265-273, March/April. 1989.

[3] W.L.Soong, and T.J.Miller, "Field-weakening performance of brushless synchronous AC motor drives," *IEE Proc.-Electr. Power Appl.*, vol. 141, no.6 pp 331-339, November 1994.

[4] T.M.Jahns, "Flux-weakening regime operation of an interior permanent-magnet synchronous motor drive," *IEEE Trans. Ind. Appl.*, vol. IA-23, pp 681-689, July/Aug. 1987.

[5] R.Dhaouadi, and N.Mohan, "Analysis of current-regulated voltage-source inverters for permanent magnet synchronous motor drives in normal and extended speed ranges," *IEEE Trans. on Energy conversion,* vol. 5, no.1, pp 137-144, March. 1990.

[6] S.D.Sudhoff, K.A.Corzine, and H.J.Hegner, "A flux-weakening strategy for current-regulated surface-mounted permanent-magnet machine drives," *IEEE Trans. on Energy Conversion,* vol. 10, no.3 pp 431-437, September 1995.

[7] S.R.Macminn, and T.M.Jahns, "Control techniques for improved high-speed performance of interior PM synchronous motor drives," *IEEE Trans. Ind. Appl.,* vol. IA-27, pp 997-1004, Sept./Oct. 1991.

[8] C.C.Chan, J.Z.Jiang, W.Xia, and K.T.Chau, "Novel wide range speed control of permanent magnet brushless motor drives," *IEEE Trans. on Power Electronics,* vol. 10, no.5, pp 539-546, September 1995.

[9] P.Stewart, V. Kadirkamanathan, "On steady-state and dynamic performance of model reference control for a permanent magnet synchronous motor". *UKACC International Conference on Control '98, Swansea, UK* No. 455, pp 664-669, IEE1998, 1-4 Sept 1998.

[10] L.R.Hunt,R.Su, and G.Meyer, "Design for multi-input non-linear systems," *Burkhauser, New York,* Differential Geometric Control Theory, pp 268-298, 1983.

[11] S.Morimoto, M.Sanada, and Y.Takeda, "Wide-speed operation of interior permanent magnet synchronous motors with high-performance current regulator," *IEEE Trans. Ind. Appl.,* vol. IA-30, no.4, pp 920-926, July/Aug. 1994.